Blue-Shifting C−H···X (X = O, Halogen) Hydrogen Bonds in the Dimers of Formaldehyde Derivatives

Attila Kovács,*,† Andrea Szabó,‡ Dénes Nemcsok,‡ and István Hargittai‡,§

Research Group for Technical Analytical Chemistry of the Hungarian Academy of Sciences at the Institute of General and Analytical Chemistry, Budapest University of Technology and Economics, H-1111 Budapest, Szt. Gellért tér 4, Hungary, Institute of General and Analytical Chemistry, Budapest University of Technology and Economics, H-1111 Budapest, Szt. Gellért tér 4, Hungary, and Structural Chemistry Research Group of the Hungarian Academy of Sciences at Eötvös University, POB 32, H-1518 Budapest, Hungary

Received: February 12, 2002; In Final Form: April 18, 2002

The potential energy surface (PES) of the dimers of formaldehyde derivatives CH(O)Y (Y = H, CH_3, F, Cl, Br, I) has been investigated by means of quantum chemical calculations at the MP2/6-311++G** level. Several minima have been found on the PES characterized by various combinations of C−H···X (X = O, halogen) contacts. The computed dimerization energies revealed the importance of dispersion forces in the formation of $[CH(O)Y]_2$ dimers, while only a lesser role of the intermolecular H···X interactions. The most characteristic geometrical properties of the dimers are the H···X distances being near the sum of the van der Waals radii of the contacting atoms, the lengthening of the contacting C−X bonds, and the general shortening of the C−H bonds by 0.001−0.004 Å with respect to the monomers. The latter bond shortening is responsible for the characteristic blue-shift of the CH stretching frequencies in the dimers. A natural bond orbital (NBO) analysis revealed a slight decrease in the population of the contacting σ^*_{CH} orbitals and alterations in the intramolecular charge-transfer effects as the primary reason of the C−H contraction.

Introduction

Hydrogen bonding (HB) belongs to the most important weak interactions in nature being intimately involved in the structure and properties of water in its various phases, in large molecules such as proteins and nucleic acids, as well as in solvation processes and the functioning of enzymes.[1,2] Most hydrogen bonds are of YH···X type, where Y is an electronegative atom and X is either an electronegative atom having one or more lone electron pairs (e.g., O, N, halogens) or a region of excess electron density like aromatic π-systems.[1] In addition to these well-known types of HB, other characteristic, although weaker, interactions may appear between a CH hydrogen and an X acceptor.[2,3]

The C−H···X interactions follow the properties of the more conventional YH···X ones, although to a lesser degree. The most common structural and spectroscopic changes such as the lengthening of the Y−H bond and the red-shift of the YH stretching frequency have been observed in most C−H···X systems.[2] An intriguing observation was made in 1989 when a small (7 cm^{-1}) blue-shift of the chloroform CH stretching frequency was found in the IR spectrum of triformylmethane in $CHCl_3$. It was attributed to intermolecular HB of $CHCl_3$ with the solute molecules.[4] The second experimental indication of blue-shifting hydrogen bonds came eight years later:[5] The IR spectra of chloroform, deuteriochloroform, and bromoform mixed with various proton acceptors, such as carboxy, nitro, and sulfo compounds, showed CH/CD stretching frequencies of the haloform higher by 3−8 cm^{-1} as compared to those in the absence of the proton acceptors. Theoretical calculations indicated C−H bond shortening in CH_4···FH,[6] CH_4···OH_2,[7] and various H_2C−H···O═C systems.[8] Subsequent spectroscopic and theoretical investigations pointed to a more frequent occurrence of this phenomenon than previously supposed.[9−14] It was named "improper, blue-shifting hydrogen bonding".[15]

To rationalize the C−H bond shortening and the consequent blue-shift of the CH stretching frequency, two explanations have been suggested. Hobza et al. called attention to the unusual hyperconjugation effect in these derivatives. In the common red-shifting hydrogen bonds a considerable charge transfer occurs from X to the antibonding σ^* orbital of the Y−H bond resulting in an increase of this bond distance.[16] In blue-shifting HB systems an analogous population increase in the σ^* orbital of the contacting C−H bond could not be observed. Instead, the charge transfer is directed toward other orbitals in the remote moiety of the hydrogen-bonded complex, in most known examples to σ^* orbitals of C−Hal bonds or to lone pairs of electrons on halogen atoms. The C−H contraction was suggested to be the consequence of a subsequent structural re-organization in the remote moiety of the complex.[15] Recently, another explanation for the C−H bond shortening, the effect of the electric field exerted by the proton acceptor molecule, was suggested.[17] In fact, ab initio calculations on methane at the HF/D95** level revealed a slight shortening of the C−H bond reaching its greatest extent at an applied field of about 0.02 au.[17]

The goal of the present study is the analysis of C−H···X (X = O, halogen) hydrogen bonds in the dimers of formaldehyde derivatives. Of these compounds, the dimers of formaldehyde

* Corresponding author. E-mail: akovacs@mail.bme.hu.

† Research Group for Technical Analytical Chemistry of the Hungarian Academy of Sciences at the Institute of General and Analytical Chemistry, Budapest University of Technology and Economics.

‡ Institute of General and Analytical Chemistry, Budapest University of Technology and Economics.

§ Structural Chemistry Research Group of the Hungarian Academy of Sciences at Eötvös University.

10.1021/jp020427n CCC: $22.00
Published on Web 05/21/2002

and acetaldehyde have been investigated. The structure of the formaldehyde dimer was determined in the gas phase by Lovas et al.[18] by means of pulsed beam microwave spectroscopy. Theoretical studies were in agreement with the reported experimental structure and indicated the possibility of other minima on the potential energy surface (PES) of the dimer.[19−22] The blue-shift of the CH stretching frequency in the formaldehyde dimer was observed rather early, but was interpreted first as incompatible with a hydrogen-bonded structure.[23−25] Quantum chemical computations, however, revealed the existence of weak C−H···O hydrogen bonds in the dimer characterized by a slight shortening of the contacting C−H bond and a blue-shift of the CH stretching frequency.[26] Similar blue-shifting C−H···O hydrogen bonds have been reported for the dimers of acetaldehyde.[27]

Halogen substituents on the formaldehyde skeleton represent a second proton acceptor in the molecular system giving rise to a more complex PES, i.e., to additional dimer structures possessing C−H···Hal contacts. The most interesting questions here are the properties of these C−H···Hal interactions, as well as the consequences of halogen substitution on the C−H···O interactions. Various properties of the C−H···X interactions, viz., dimerization energy, geometrical characteristics, charge distribution, and vibrational frequencies have been determined by quantum chemical computations. They are well suited to scan the complete PES, to determine the molecular properties of both the global and local minimum structures, and to provide consistent data for a set of related molecules. The choice of the method of computation is crucial: proper treatment of electron correlation and large diffuse basis sets are the basic requirements for studies of weak interactions. Among the correlated methods, the MP2 level is superior over density functional theory (DFT) for such studies [27−29] because DFT does not account for the London dispersion energy.[30]

Computational Details

The calculations were carried out using the second-order Møller-Plesset perturbation theory in the frozen-core approximation (MP2)[31] in conjunction with diffuse polarized valence double- and valence triple-ζ basis sets. The initial geometry optimizations and frequency calculations were performed using the 6-31++G** basis as implemented in Gaussian 98[32] except for iodine for which a quasi-relativistic effective core potential (ECP) with a (31/311/1) valence basis was applied.[33,34]

The final energetic and structural characterization of the dimers was carried out using the 6-311++G** basis set. For bromine, this basis set keyword in Gaussian 98 refers to the (631111111/33311111/411) basis. Additionally, in these calculations the previous valence basis of iodine was extended with a single set of *sp* diffuse functions ($\alpha = 0.035$). Analysis of the charge distribution and charge-transfer processes was performed using the NBO partitioning scheme[16] while the basis set superposition error was calculated according to the counterpoise method.[35] In all the calculations the Gaussian 98 program[32] extended by the NBO 5.0 code[36] was used.

Results and Discussion

Monomers. Selected computed data, viz., bond distances, atomic charges, dipole moments, and polarizabilities of the monomers are compiled in Table 1. To assess the quality of the theoretical data, experimental geometrical parameters available for formaldehyde,[37] acetaldehyde,[38] CH(O)F,[39] and CH(O)Cl[40] are also included in Table 1. Keeping in mind the difference in the physical meaning of the computed and experimental results,[41] there is good agreement between the theoretical and experimental geometries. The C−F distance appears overestimated by about 0.01 Å by the computations.

TABLE 1: Selected Molecular Properties of Formaldehyde Derivatives CH(O)Y

	Y					
parameter	H	CH_3	F	Cl	Br	I
			Computed[a]			
r_{C-O}	1.213	1.215	1.185	1.191	1.189	1.188
r_{C-Y}		1.505	1.351	1.764	1.946	2.182
r_{C-H}	1.105	1.110	1.094	1.097	1.097	1.099
q_O	−0.467	−0.492	−0.473	−0.443	−0.432	−0.430
q_Y			−0.361	−0.057	−0.036	+0.015
q_H	+0.088	+0.081	+0.102	+0.127	+0.133	+0.137
q_C	+0.395	+0.424	+0.732	+0.373	+0.335	+0.279
μ	2.392	2.764	2.121	1.878	1.817	1.710
α[b]	15.257	27.746	15.715	26.630	33.532	45.940
			Experimental[c]			
r_{C-O}	1.206(3)	1.213(10)	1.181(5)	1.1820(50)		
r_{C-Y}		1.504(10)	1.338(5)	1.7650(30)		
r_{C-H}	1.108(4)	1.106(5)	1.095(10)	1.0897(50)		

[a] The geometrical parameters (r, in angstrom), natural atomic charges (q, in au), dipole moments (μ, in Debye) and polarizabilities (α, in au) were calculated at the MP2/6-311++G** level. [b] The α values were obtained from the computed polar tensors according to $\alpha = 1/3(\alpha_{xx} + \alpha_{yy} + \alpha_{zz})$.[53] [c] The experimental data were taken from the following references: CH_2O (r_s);[37] $CH(O)CH_3$ (r_a);[38] CH(O)F (r_s);[39] CH(O)Cl (r_e).[40] Experimental errors are given in parentheses.

The charge distribution in the monomers is of primary importance from the point of view of the C−H···X interaction. The atomic charges in the formaldehyde derivatives are in agreement with the electron withdrawing/donating properties of the substituents. Thus, the CH hydrogen is most acidic in the halo-derivatives while it is the least acidic in acetaldehyde (cf. Table 1). Similarly, the oxygen has the largest negative charge in acetaldehyde while its charge gradually decreases in the halogen derivatives. We note the small magnitude of the halogen atomic charges (except for fluorine) and the slightly positive charge of iodine in these compounds. As expected, the fluorine has a considerable negative charge, but it is still smaller, by about 0.1 *e* than that of oxygen. This observation suggests that the strongest C−H···X interactions should be formed with the oxo group, while those with halogens will be weaker. An additional interesting trend in the atomic charges is the increasing acidity of the CH hydrogen from the fluoro to the iodo derivatives. This is paralleled by the decreasing polarized character of the C═O and C−Hal bonds.

On the basis of the computed dipole moments and polarizabilities of the monomers (Table 1) we can make some assumptions on the van der Waals interactions in the dimers. The strongest dipole−dipole interactions can be expected in the formaldehyde and acetaldehyde dimers, and the magnitude of this interaction decreases toward the iodo derivative. On the other hand, the dispersion forces (originating from interactions of induced dipoles and being proportional to the polarizabilities) will be the largest in the dimers of CH(O)I and CH(O)Br and the weakest in the dimers of CH_2O and CH(O)F.

Dimers. The search of the PES of the dimers resulted in eight different minimum structures depicted in Figure 1. They can be distinguished by the type of C−H···X contacts and relative orientation of the monomer planes. Two somewhat different dimer structures with a single C−H···O contact have been found. In structures **I** (X = Cl, Br, I) the two C−H bonds are nearly perpendicular, while in structure **II** (X = F) they are nearly in line. We note that related dimer structures possessing a single C−H···Hal contact could not be found, in agreement

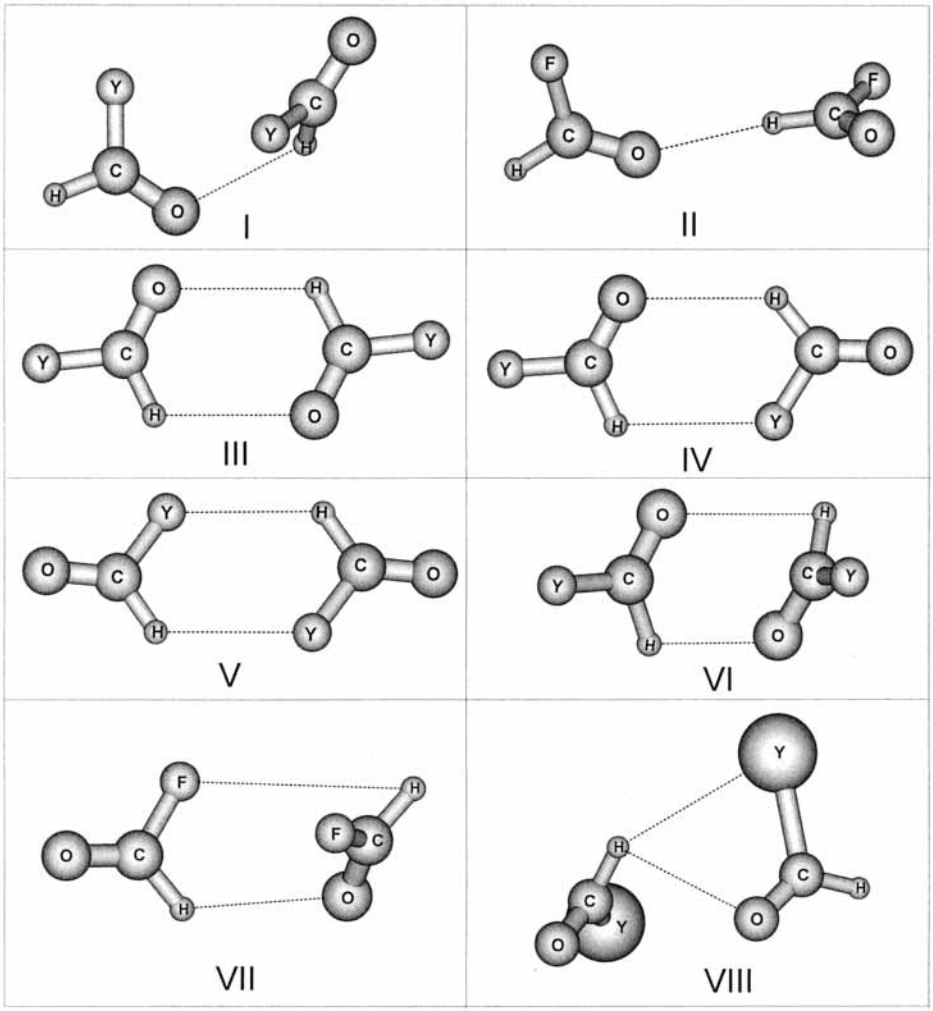

Figure 1. Optimized structures of the possible dimers of formaldehyde derivatives.

with the proposed weaker proton acceptor ability of the halogens (vide supra). Similarly, neither dimers **I** or **II** were found for formaldehyde and acetaldehyde due to the preference of bifurcated C−H···O···H−C interactions in these derivatives. The formation of single-contact structures among the halogen−formaldehyde dimers is the obvious consequence of the lack of a second hydrogen in the monomers.

Additional dimers include three coplanar structures with double C−H···X interactions: the symmetric ones with X = O (**III**) and X = halogen (**V**) and the asymmetric one with X = O/halogen (**IV**). Double C−H···X contacts but with near perpendicular planes of the monomers are present in structures **VI** and **VII**. The latter one with the mixed C−H···O/Hal contact was found only for CH(O)F. The arrangement of the monomers in dimer **VIII** (found only for CH(O)Br and CH(O)I) is close to that of dimer **I**, but the hydrogen is involved in a bifurcated interaction with O (at 2.710 and 2.739 Å) and Br (3.064 Å) and I (3.237 Å), respectively, of the other moiety. We note the first-order saddle-point character of structure **III** of $[CH(O)Cl]_2$, which dimer is strongly preferred for the other formaldehydes. That some dimer structures do not appear uniformly for all the halogen−formaldehydes[42] may be somewhat surprising. It may be attributed to differences in local interactions. In the following discussion we will focus mainly on the most frequent structures.

The computed dimerization energies are compiled in Table 2. For the sake of consistency, we computed (and included) the respective data of the analogous dimers of formaldehyde and acetaldehyde. This check was necessary, because recently dimerization energies of ca. 50 kJ/mol have been reported for formaldehyde dimers,[26] which would mean extremely strong HB interactions, unlikely for a CH hydrogen. On the other hand, the literature[27,43] and our dimerization energies for dimer **II** of acetaldehyde are in fair agreement. Interaction energies of similar magnitude have also been reported for the acetone dimer[44] and for $(NH_3)_2$.[45]

TABLE 2: Computed Dimerization Energies (kJ/mol)[a]

Y	I	II	III	IV	V	VI	VII	VIII
H			−9.9			−10.6		
CH_3			−11.6					
F		−8.5	−13.2	−10.9	−8.4	−11.9	−9.7	-
Cl	−13.3			−13.3	−9.8	−14.9		
Br	−12.3		−11.1	−11.7	−9.9	−12.2		−11.5
I	−15.2		−16.5	−15.7	−15.5	−16.5		−15.2

[a] Computed at MP2/6-311++G** level and corrected for ZPE (from MP2/6-31++G** harmonic frequency analysis, scaled by 0.9608[54]). For the structures of dimers **I**−**VIII** see Figure 1.

Before a detailed discussion of the computed properties we comment on the reliability of these data. A crucial point in the study of weak interactions is the quality of basis sets. Basis sets not large enough can give rise to two kinds of errors: (i) They may not account properly for the London dispersion forces and hence underestimate the interaction energy. (ii) They are accompanied by large BSSE, which acts in the opposite direction, and strengthens the interaction in the model artificially. When correcting for BSSE, a further uncertainty comes from a

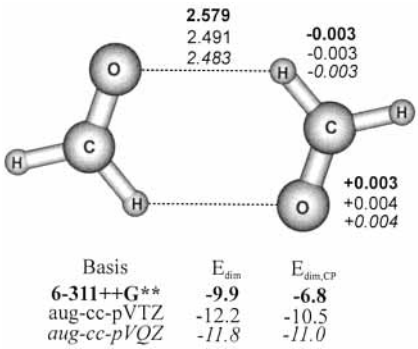

Figure 2. Basis set dependence of the computed dimerization energy (uncorrected, E_{dim}, and BSSE corrected $E_{dim,CP}$, kJ/mol) and geometrical characteristics (intermolecular distance, shortening of the C−H, and lengthening of the C═O bonds, Å) for the formaldehyde dimer **III**.

principal deficiency of the popular counterpoise (CP) method,[46,47] from its overestimation of BSSE.[48] Moreover, while the interaction energies are believed to be corrected more or less for BSSE, the geometrical consequences of the overestimated interaction (e.g., shorter intermolecular distance) remain unchanged in the usual CP procedure.[49,50] This latter error is proportional to the magnitude of BSSE with respect to the total interaction energy.[50]

Unfortunately, the size of the dimers and the available basis sets for the heavy atoms limited our choice for basis set. In weak hydrogen-bonded complexes the BSSE of the MP2/6-311++G** level was found to be 30−50% of the interaction energy.[51] To assess the error of our computed data we performed test calculations on structure **III** of the formaldehyde dimer at the MP2/aug-cc-pVTZ and MP2/aug-cc-pVQZ levels. The latter basis has been found to converge satisfactorily to saturation for weak interactions.[45]

Figure 2 illustrates the dimerization energy and selected geometrical properties of the formaldehyde dimer **III** as obtained by using the 6-311++G**, aug-cc-pVTZ, and aug-cc-pVQZ basis sets. Our first conclusion is the importance of the augmented diffuse basis set for an accurate description of the van der Waals interaction. This is well seen in both the uncorrected dimerization energies (increased by 2 kJ/mol) and in the H···O distances (decreased by 0.1 Å), as compared with the MP2/6-311++G** values. These data indicate that the main deficiency of the 6-311++G** basis set in our case is in its underestimating the dispersion interactions. The opposite effect of BSSE did not sufficiently compensate for this. Moreover, the CP correction further increased the error of the MP2/6-311++G** dimerization energy. Therefore, the uncorrected MP2/6-311++G** energies seemed to us to be a better measure of the effects investigated here than the CP-corrected ones, even though they may still be somewhat underestimated. The changes of the C−H and C═O bond lengths upon dimer formation as obtained from the MP2/6-311++G** computations appear reliable enough for our forthcoming discussion.

van der Waals dimers are stabilized by competing electrostatic, induction, charge-transfer, and dispersion energy contributions, while the exchange interaction energy accounts for the repulsive forces in accordance with the Pauli principle.[52] In weakly bound complexes with large intermolecular distances, the London dispersion forces are believed to provide the largest attractive contribution to the interaction energy. Table 2 reveals close interaction energies for the dimer structures in the CH(O)Y series. The energies are especially close (within 2 kJ/mol) for $[CH(O)Br]_2$ and $[CH(O)I]_2$, where the greatest dispersion interactions are expected. Considering, that a H···O interaction should be much stronger than a H···Br or H···I one, the close interaction energies of the dimers with H···O and H···Br (or H···I) contacts suggest that the local C−H···X interactions have only a minor role in them. On the other hand, the C═O and C−Hal bonds are more polarized in CH(O)F and CH(O)Cl than in their bromine and iodine analogues (vide supra) resulting in stronger local H···X interactions in their dimers. The variation in polarization may then be responsible for the somewhat more pronounced differences in the relative stabilities among the structures in each of the $[CH(O)F]_2$ and $[CH(O)Cl]_2$ series of models.

Although the local H···X interactions play a minor role in the stability of the dimers, some trends can be discerned. Generally, the C−H···O contacts are slightly preferred over the C−H···Hal ones. This observation is supported by the intermediate dimerization energies of structures **IV** characterized by mixed C−H···O/Hal contacts. Most single-contacted dimers are less preferred than the double-contacted ones, but the energy differences are rather small, in agreement with the lesser importance of the local C−H···X interactions. As predicted by the computed polarizabilities of the monomers (vide supra), the largest dimerization energies were obtained for the $[CH(O)I]_2$ dimers, while the smallest for $(CH_2O)_2$ and $[CH(O)F]_2$. The relative stabilities of the $[CH(O)Cl]_2$ and $[CH(O)Br]_2$ dimers seem to deviate slightly from the trend predicted by the computed polarizabilities. We recall, however, that basis set dependence of the interaction energy may be responsible for minor deviations.

Geometrical Characteristics of the H···X Interactions. The geometrical data of the dimers give information on the local H···X interactions. The most characteristic parameters are the nonbonded H···X distances and H···X−C angles as well as the changes in the lengths of the C−H and C−X bonds upon the interaction. Selected data from the MP2/6-311++G** calculations are compiled in Table 3. As was shown above, the H···X distances are somewhat overestimated at this level of theory. Expecting consistency in the magnitude of errors, this may not influence the following conclusions considerably. On the other hand, the changes in the C−H and C−X bonds proved to be reliable within the required accuracy (vide supra).

In agreement with the weak character of the local interactions, the H···X distances are close to the sum of the van der Waals radii (ΣvdW) of the contacting atoms. The H···O distances are the shortest in the single-contacted **I** and **II**, being by 0.2−0.3 Å below ΣvdW (cf. Table 3). Similar H···O distances appear in structures **IV**, indicating that the strongest H···O interactions occur in these three structures. The H···O distances are near ΣvdW in structures **III** and, partly, in structures **VI**. Note that the other (longer) H···O contacts in **VI** exceed ΣvdW by 0.3−0.5 Å. The H···Hal nonbonded distances agree with ΣvdW in structures **IV**, while they decrease gradually from ΣvdW when going from F to I in structures **V**. The latter feature is the most characteristic geometrical indicator of the increasing dispersion forces with the larger polarizability of the heavier CH(O)Y species.

The most favored H···X contacts occur when H approaches X at its most electron-rich site, i.e., from the direction of the lone pairs. Accordingly, the H···O−C angles in structures **I** are around 110°. The corresponding angle in the similarly single-contacted structure **II** of $[CH(O)F]_2$ is 146.2°. The increase may be attributed to the larger electrostatic repulsion between fluorine of the proton acceptor and the negative centers of the proton donor moiety. In structures **III**−**VI** the nonbonded H···O−C and H···Hal-C angles deviate up to 20° from the optimal value due to the geometric constraints of the double H···X contact.

TABLE 3: Computed[a] Geometrical Characteristics of C−H···X (X = O, halogen) Interactions in Selected $[CH(O)Y]_2$ Dimers

Y	parameter[b]	I/II[c]	III	IV	V	VI[d]
H	H···O (2.60)	-	2.579	-	-	2.896/2.480
	Δ(C═O)		+0.003			+0.003/+0.002
	Δ(C−H)		−0.004			−0.002/−0.002
CH_3	H···O (2.60)	-	2.533	-	-	-
	Δ(C═O)		+0.004			
	Δ(C−H)		−0.004			
F	H···O (2.60)	2.369	2.562	2.511	-	3.110/2.651
	H···F (2.55)	-	-	2.576	2.549	-
	Δ(C═O)	+0.002	+0.003	+0.003		+0.002/+0.002
	Δ(C−F)			+0.015	+0.012	
	Δ(C−H)	−0.002	−0.002	−0.001[e]/−0.002[f]	−0.002	−0.002/−0.001
Cl	H···O (2.60)	2.370	-	2.371	-	2.971/2.571
	H···Cl (3.00)	-		3.038	2.857	-
	Δ(C═O)	+0.002		+0.004		+0.003/+0.002
	Δ(C−Cl)			+0.021	+0.017	
	Δ(C−H)	−0.002		−0.001[e]/−0.003[f]	−0.002	−0.002/−0.001
Br	H···O (2.60)	2.435	2.553	2.336	-	2.919/2.617
	H···Br (3.15)	-	-	3.143	2.919	-
	Δ(C═O)	+0.002	+0.003	+0.004		+0.003/+0.001
	Δ(C−Br)			+0.025	+0.023	
	Δ(C−H)	−0.001	−0.001	0.000[e]/−0.002[f]	−0.001	−0.001/+0.001
I	H···O (2.60)	2.376	2.544	2.293	-	2.885/2.656
	H···I (3.35)	-	-	3.278	3.027	-
	Δ(C═O)	+0.003	+0.003	+0.005		+0.004/+0.001
	Δ(C−I)			+0.030	+0.030	
	Δ(C−H)	−0.001	−0.001	−0.001[e]/−0.001[f]	−0.001	−0.002/0.000

[a] Computed at the MP2/6-311++G** level. [b] The H···X nonbonded distances and changes in the bond lengths of the contacting atoms with respect to the monomers are given in angstroms. Values in parentheses represent the sum of the van der Waals radii of the contacting atoms. [c] Structure **II** for Y = F. [d] The first values refer to the upper C−H···O contact, while the second values to the bottom one in Figure 1. [e] The C−H bond contacted to Hal (cf. Figure 1). [f] The C−H bond contacted to O (cf. Figure 1).

The H···X interactions result in characteristic changes of the geometrical parameters as compared to the unperturbed ones of the monomers. The elongation of the C═O and C−Hal bonds participating in the contact is the most noteworthy change (cf. Table 3). This amounts to 0.003 Å for the C═O bond and is in the range of 0.012(F)−0.030(I) Å for the C−Hal bonds. The conspicuous elongation of the C−Hal bonds may be explained by the flexibility of a single bond as compared to the C═O double bond. The trend of elongation increasing from F to I is in agreement with the decrease of the H···Hal intermolecular distances with respect to ΣvdW. The noncontacting C═O and C−Hal bonds decrease upon dimer formation except for the C−Hal bonds of structures **I** and **II**, for which an increase of 0.01−0.02 Å is observed. As characteristic for blue-shifting HB, the contacting C−H bonds show a slight (0.001−0.002 Å) shortening. This property will be discussed in the next section.

Blue-Shifting Hydrogen Bonds. The frequency analysis revealed the blue-shifting character of the C−H···X interactions in the dimers. In agreement with the computed C−H bond contraction, the CH stretching frequencies of the contacting CH groups were higher by 6−33 cm^{-1} in the dimers than the respective frequencies of the monomers. However, the individual blue-shifts cannot be correlated directly to the magnitude of C−H contraction, because most of the CH stretching modes consist of a mixture of the two C−H internal coordinates.

To elucidate the origin of the C−H bond contraction, we analyzed the charge distribution properties of the dimers. The natural atomic charges of the contacting atoms in selected dimers are compiled in Table 4. To become a better electron donor, the proton acceptor oxygen and halogens gain charge in the dimer: the oxygens between 20 and 30 me, while the halogens from 20 me (F) up to 58 me (I) as compared to the monomers. On the other hand, the contacting hydrogen atoms lose charge (10−20 me) in all cases. This means that the contacting bonds become more polarized in the dimers, whereby promoting the proton donor−acceptor interaction. The contacting bonds have an enhanced polarized character in structures **IV** as compared with the symmetric double-contacted structures **III** and **V**.

TABLE 4: Computed[a] Natural Charges of the Contacting Atoms in Selected $[CH(O)Y]_2$ Dimers

Y	atom	I/II[b]	III	IV	V	VI[c]
H	O	-	−0.490	-	-	−0.483/−0.507
	H		0.112			0.091/0.108
CH_3	O	-	−0.515	-	-	-
	H		0.110			
F	O	−0.494	−0.499	−0.496	-	−0.492/0.498
	F	-	-	−0.381	−0.379	-
	H	0.123	0.120	0.114[d]/0.125[e]	0.117	0.110/0.114
Cl	O	−0.461	-	−0.472	-	−0.464/−0.470
	Cl	-		−0.098	−0.086	-
	H	0.144		0.135[d]/0.153[e]	0.139	0.135/0.139
Br	O	−0.453	−0.459	−0.466	-	−0.454/−0.457
	Br	-	-	−0.085	−0.076	-
	H	0.150	0.149	0.143[d]/0.159[e]	0.148	0.142/0.143
I	O	−0.453	−0.458	−0.468	-	−0.453/−0.451
	I	-	-	−0.043	−0.037	-
	H	0.151	0.152	0.146[d]/0.162[e]	0.153	0.146/0.144

[a] Computed at the MP2/6-311++G** level. [b] Structure **II** for Y = F. [c] The first values refer to the upper C−H···O contact, while the second values refer to the bottom one in Figure 1. [d] The C−H bond contacted to Hal (cf. Figure 1). [e] The C−H bond contacted to O (cf. Figure 1).

The net charge transfer (CT) from the proton acceptor toward the proton donor moiety could be evaluated only in structures **I** and **II** utilizing the computed natural charges. It has a similar magnitude for the four halogen-formaldehydes corresponding to 5.1, 4.1, 5.2, and 6.5 me in $[CH(O)F]_2$, $[CH(O)Cl]_2$, $[CH(O)Br]_2$, and $[CH(O)I]_2$, respectively.

TABLE 5: Characteristics of Charge Transfer Interactions in $[CH(O)Br]_2$ Dimers

parameter[a]	I	III	IV[b]	V	VI[c]
			Intermolecular		
$E^{(2)}$ $n_{1O} \rightarrow \sigma^*_{CH}$	2.5	0.9	4.1	-	0.5
$E^{(2)}$ $n_{2O} \rightarrow \sigma^*_{CH}$	2.2	1.1	5.4	-	0.3
$E^{(2)}$ $n_{1Br} \rightarrow \sigma^*_{CH}$	-	-	0.6	1.4	-
$E^{(2)}$ $n_{2Br} \rightarrow \sigma^*_{CH}$	-	-	1.9	9.2	-
			Intramolecular		
$\Delta E^{(2)}$ $n_{2O} \rightarrow \sigma^*_{CH}$	−9.1	−8.0	−11.7/−6.3	−7.6	−6.7
$\Delta E^{(2)}$ $n_{2O} \rightarrow \sigma^*_{CBr}$	+15.0	−7.4	+30.6/−15.3	+24.8	−13.6
$\Delta E^{(2)}$ $n_{2Br} \rightarrow \sigma^*_{CH}$	−1.3	+0.2	−2.6/+0.7	−3.1	+0.5
$\Delta E^{(2)}$ $n_{2Br} \rightarrow \sigma^*_{CO}$	−2.7	+0.8	−2.3/+0.5	−1.63	+1.3
$\Delta E^{(2)}$ $n_{3Br} \rightarrow \pi^*_{CO}$	−22.7	+4.8	−9.7/+8.5	−9.9	+5.3
$\Delta\sigma^*_{CH(\cdots O)}$	−2.9	−3.3	−4.4	-	−1.1
Δ(C−H)	−0.001	−0.001	−0.002		0.0
$\Delta\sigma^*_{CH(\cdots Br)}$	-	-	−0.8	−0.2	-
Δ(C−H)			0.0	−0.001	
$\Delta\sigma^*_{CBr}$	+12.8[d]	−7.5	−14.1	-	−13.2
Δn_{Br}	+6.6[d]	−5.0	−9.8		−7.1
Δ(C−Br)	+0.016[d]	−0.006	−0.013		−0.011
$\Delta\sigma^*_{CBr(\cdots H)}$	-	-	+21.2	+20.1	-
$\Delta n_{Br(\cdots H)}$			−9.8	+4.3	
Δ(C−Br)			+0.025	+0.023	
$\Delta\sigma^*_{CO(\cdots H)}$	+0.7	+0.5	+1.0	-	+0.6
$\Delta\pi^*_{CO(\cdots H)}$	+0.3	+2.2	+5.6		+5.3
$\Delta n_{O(\cdots H)}$	+6.4	+10.0	+12.4		+3.3
Δ(C=O)	+0.002	+0.003	+0.004		+0.001
$\Delta\sigma^*_{CO}$	−0.5	-	−0.9	−1.0	-
$\Delta\pi^*_{CO}$	−5.4		−9.9	−8.8	
Δn_O	−7.0		−13.0	−13.4	
Δ(C=O)	−0.002		−0.003	−0.003	

[a] The second-order perturbation energies ($E^{(2)}$ donor → acceptor, kJ/mol) were obtained from HF/6-311++G** single-point calculations on the MP2/6-311++G** geometries; the change in the population of the given orbitals (me) were obtained from MP2/6-311++G** calculations. The bond length changes are given in Å. [b] The first values in the data pairs refer to the unit with C−H bond contacted to O, while the second ones to the unit with C−H bond contacted to Br (cf. Figure 1). [c] The data refer to the monomer, of which H forms the shortest C−H···O contact. [d] The data refer to the monomer, of which H forms the C−H···O contact.

More detailed information on the CT processes can be obtained by investigating the change in the occupation of the acceptor and donor natural bond orbitals and the delocalization processes upon dimer formation. The delocalization effects can be identified from the off-diagonal elements of the Fock matrix in the NBO basis. The strengths of these interactions are estimated by second-order perturbation theory.[16] The second-order perturbation energies, $E^{(2)}$, corresponding to the intermolecular $n_O \rightarrow \sigma^*_{CH}$ and $n_{Br} \rightarrow \sigma^*_{CH}$ CTs as well as the change of the most important intramolecular $E^{(2)}$-s and natural orbital populations upon dimer formation for the $[CH(O)Br]_2$ dimers are compiled in Table 5. Analogous data were obtained for the respective dimers of the other halogen-formaldehydes.

In HB interactions the intermolecular CT occurs between the lone pairs of X (electron donor) and the σ^*_{CH} antibond of the contacting hydrogen (electron acceptor). Among these lone pairs n_1 has the lowest while n_3 the highest orbital energy. According to the data of Table 5 the magnitude of CT seems to be hardly dependent on the type of X, rather, it is strongly related to the H···X distance. The strongest interactions can be observed with O of **IV** and Br of **V**, possessing the shortest H···X contacts as compared with the respective ΣvdW values (cf. Table 3). Note, that while the two lone pair orbitals of O donate the charge in a similar amount, the donation from n_2 of the halogen exceeds considerably that from n_1.

The most important intramolecular delocalization effects in CH(O)Br are $n_{2O} \rightarrow \sigma^*_{CH}$, $n_{2O} \rightarrow \sigma^*_{CBr}$, $n_{2Br} \rightarrow \sigma^*_{CH}$, $n_{2Br} \rightarrow \sigma^*_{CO}$, and $n_{3Br} \rightarrow \pi^*_{CO}$ with second-order perturbation energies of 110.2, 234.4, 12.7, 27.6, and 91.8 kJ/mol, respectively, in the monomer. The dimer formation alters the magnitude of CT between the lone pair and antibonding orbitals resulting in characteristic changes in the population of the interacting orbitals. There is a good correlation between these changes and the changes in the respective bond distances upon dimer formation. Hence, the population decrease of σ^*_{CH} can be associated with the contraction of the C−H bond (cf. Table 5), being the primary reason of the blue-shifting effect.

The CT interactions in the single-contacted dimers differ considerably from those in the double-contacted ones. In **I**, the charge transferred from the proton acceptor monomer (5.2 me) is accumulated on the σ^*_{CBr} and n_{Br} orbitals of the proton donor monomer. In addition to the intermolecular CT, however, the population increase of σ^*_{CBr} has an important contribution from n_{2O}, while that of n_{Br} gains additionally from the decrease of $n_{3Br} \rightarrow \pi^*_{CO}$ interactions. The geometrical consequence of this complex CT process is the well-defined lengthening of the C−Br bond in the proton donor moiety. Thus, dimers **I(II)** show characteristics similar to those observed for other (single-contacted) blue-shifting HB systems.[15]

A different picture appears, however, in the double-contacted structures, where the noncontacting C−Hal bond (**III**, **IV**, **VI**) shortens upon dimer formation while the C−H bonds show the same shortening effect as before (cf. Table 3). Analysis of delocalization in these dimers reveals a decrease of both the σ^*_{CBr} and n_{Br} populations due to a decrease of the $n_{2O} \rightarrow \sigma^*_{CBr}$ and increase of the $n_{3Br} \rightarrow \pi^*_{CO}$ interactions (cf. Table 5). The opposite effects can be observed on the bromines contacted to H in structures **IV** and **V**, resulting in the characteristic elongation of the C−Br bond upon HB. Apparently, in the double-contacted structures the CT is directed toward the proton acceptor X instead of the remote one, supporting the local H···X interaction by an increase of the lone pair orbital population and by elongating the C−X bond.

Prompted by the recent results of Masunov et al.[17] we checked also the effect of electric field on the geometrical properties. According to our computations the formaldehyde derivatives generate an electric field of ca. 0.005 au in a range of 4 Å, the distance between the monomer centers in the dimers. To determine its geometrical consequences we performed a scan of the monomers' PES at the MP2/6-311++G** level applying the above electric field. The C−H bond was placed both parallel and perpendicular to direction of the electric field (corresponding to the C → H vector in the former case), respectively. The changes in the C−H and C−Y bond distances with respect to the unperturbed monomers are compiled in Table 6. The data show a well-defined shortening of the C−Hal bonds, its magnitude increasing from F to I (up to 0.03 Å). There are smaller changes in the C=O and C−H bonds; they lengthen upon the increase of the electric field. The effect is larger when the electric field is perpendicular to the C−H bond. A C−H bond shortening was observed only in formaldehyde and it amounted to 0.001 and 0.003 Å when the electric field was placed parallel and perpendicular to the bond, respectively (cf. Table 6). Hence the above data do not suggest an important role of the electric field in the C−H bond contraction.

Conclusions

Hydrogen-bonded complexes are stabilized mainly by electrostatic, induction, charge-transfer, and dispersion energy

TABLE 6: Changes of Selected Bond Distances (Å) of the CH(O)Y Molecules in an Electric Field of 0.005 au Placed Parallel (C → H) and Perpendicular to the C−H Bond[a]

Y	atom	⊥	II
H	C−H	−0.002	0.0
	C═O	+0.003	−0.001
CH_3	C−H	0.0	+0.003
	C═O	+0.003	0.0
	C−C	−0.004	−0.001
F	C−H	0.0	+0.001
	C═O	+0.004	−0.001
	C−F	−0.013	−0.003
Cl	C−H	0.0	+0.001
	C═O	+0.006	0.0
	C−Cl	−0.020	−0.005
Br	C−H	+0.001	+0.002
	C═O	+0.007	0.0
	C−Br	−0.025	−0.007
I	C−H	+0.001	+0.001
	C═O	+0.008	+0.001
	C−I	−0.030	−0.009

[a] Computed at the MP2/6-311++G** level.

contributions, their ratio determining the singular properties of the hydrogen bond. In complexes with large H···X distances (near the sum of the van der Waals radii of H and X) the dispersion energy contribution is the dominant one, while the local H···X interactions may play only a lesser role.

In agreement with the dominant role of the London dispersion forces, only extended diffuse basis sets describe accurately the dimer formation of formaldehyde derivatives. In MP2 calculations the error of the 6-311++G** basis is manifested in a ca. 40% underestimation of the total interaction energy. Even BSSE, acting in the opposite direction, seems to be insufficient to compensate for the former error. In contrast to strong HB systems, in the weaker complexes the parameters uncorrected for BSSE provide a better description of the molecular properties.

The survey of the PES of CH(O)Y (Y = H, CH_3, halogen) dimers resulted in eight different structures with close dimerization energies. However, some structures could not be found uniformly for all the CH(O)Y derivatives due probably to differences in the individual H···X (X = O, halogen) interactions. Of the dimers, those containing a double H···X contact are generally preferred over the single-contacted ones.

The most important geometrical consequences of dimer formation are the lengthening of the contacting C−X bonds (up to 0.030 Å of C−I) and the general shortening of the C−H bonds by 0.001−0.004 Å with respect to the monomers. The latter is responsible for the characteristic blue-shift of the CH stretching frequencies in the dimers.

As to the origin of the C−H contraction, our NBO analysis revealed a slight decrease in the population of the σ^*_{CH} orbitals upon dimer formation. Parallel to that, the intramolecular charge-transfer processes in the proton donor moiety cause marked changes: in single-contacted structures a charge concentration appears in the σ^*_{CY} and n_Y orbitals of the remote halogen, while in the double-contacted dimers similar change occurs in the σ^*_{CX} antibonding and n_X orbitals (X = O, halogen) of the contacting X. Contrary to the recent hypothesis of Masunov et al.[17] our results do not suggest an important role of the electric field for the C−H bond contraction.

Acknowledgment. This research was supported by the Hungarian Scientific Research Foundation (OTKA No. T030053) and by the Ministry of Education of Hungary (FKFP 0364/1999). Part of the computations have been performed using the SUN E10000 supercomputer of the National Information Infrastructure Development Program (NIIF). A.K. thanks the Bolyai Foundation for a fellowship.

References and Notes

(1) Jeffrey, G. A. *An Introducion to Hydrogen Bonding*; Oxford University Press: New York, 1997.

(2) Desiraju, G. R.; Steiner, T. *The Weak Hydrogen Bond*; Oxford University Press: Oxford, 1999.

(3) Green, R. D. *Hydrogen Bonding by C−H groups*; Macmillan: London, 1974.

(4) Buděšinský, M.; Fiedler, P.; Arnold, Z. *Synthesis* **1989**, 858.

(5) Boldeskul, I. E.; Tsymbal, I. F.; Ryltsev, E. V.; Latajka, Z.; Barnes, A. J. *J. Mol. Struct.* **1997**, *436*, 167.

(6) Vizioli, C. V.; Azúa, M. C. R. d.; Giribet, C. G.; Contreras, R. H.; Turi, L.; Dannenberg, J. J.; Rae, I. D.; Weigold, J. A.; Malagoli, M.; Zanasi, R.; Lazzeretti, P. *J. Phys. Chem.* **1994**, *98*, 8858.

(7) Giribet, C. G.; Vizioli, C. V.; Azúa, M. C. R. d.; Contreras, R. H.; Dannenberg, J. J.; Masunov, A. *J. Chem. Soc., Faraday Trans.* **1996**, *92*, 3029.

(8) Popelier, P. L. A.; Bader, R. F. W. *Chem. Phys. Lett.* **1992**, *189*, 542.

(9) Hobza, P.; Špirko, V.; Selzle, H. L.; Schlag, E. W. *J. Phys. Chem. A* **1998**, *102*, 2501.

(10) Hobza, P.; Špirko, V.; Havlas, Z.; Buchhold, K.; Reimann, B.; Barth, H.-D.; Brutschy, B. *Chem. Phys. Lett.* **1999**, *299*, 180.

(11) Hobza, P.; Havlas, Z. *Chem. Phys. Lett.* **1999**, *303*, 447.

(12) Gu, Y.; Scheiner, S. *J. Am. Chem. Soc.* **1999**, *121*, 9411.

(13) Reimann, B.; Buchhold, K.; Vaupel, S.; Brutschy, B.; Havlas, Z.; Špirko, V.; Hobza, P. *J. Phys. Chem. A* **2001**, *105*, 5560−5566.

(14) Sosa, G. L.; Peruchena, N. M.; Contreras, R. H.; Castro, E. A. *J. Mol. Struct. (THEOCHEM)* **2002**, *577*, 219−228.

(15) Hobza, P.; Havlas, Z. *Chem. Rev.* **2000**, *100*, 4253−4264.

(16) Reed, A. E.; Curtiss, L. A.; Weinhold, F. *Chem. Rev.* **1988**, *88*, 899.

(17) Masunov, A.; Dannenberg, J. J.; Contreras, R. H. *J. Phys. Chem. A* **2001**, *105*, 4737−4740.

(18) Lovas, F. J.; Suenram, R. D.; Coudert, L. H.; Blake, T. A.; Grant, K. J.; Novick, S. E. *J. Chem. Phys.* **1990**, *92*, 891.

(19) Del-Bene, J. E. *J. Chem. Phys.* **1974**, *60*, 3812.

(20) Kemper, M. J. H.; Hoeks, C. H.; Buck, H. M. *J. Chem. Phys.* **1981**, *74*, 5744.

(21) Zubkov, V. A. *Theor. Chim. Acta* **1984**, *66*, 295.

(22) Hobza, P.; Mehlhorn, A.; Carsky, P.; Zahradnik, R. *J. Mol. Struct. (THEOCHEM)* **1986**, *138*, 387.

(23) Khoshkhoo, H.; Nixon, E. R. *Spectrochim. Acta* **1973**, *29A*, 603.

(24) Nelander, B. *J. Chem. Phys.* **1980**, *73*, 1034.

(25) van der Zwet, G. P.; Allamandola, L. J.; Baas, F.; Greenberg, J. M. *J. Mol. Struct.* **1989**, *195*, 213.

(26) Ford, T. A.; Glasser, L. *J. Mol. Struct. (THEOCHEM)* **1997**, *398*−*399*, 381−394.

(27) Hermida-Ramón, J. M.; Ríos, M. A. *Chem. Phys. Lett.* **1998**, *290*, 431−436.

(28) Kurita, N.; Sekino, H. *Chem. Phys. Lett.* **2001**, *348*, 139−146.

(29) Kohn, W.; Becke, A. D.; Parr, R. G. *J. Phys. Chem.* **1996**, *100*, 12974.

(30) Kristyán, S.; Pulay, P. *Chem. Phys. Lett.* **1994**, *229*, 175.

(31) Møller, C.; Plesset, M. S. *Phys. Rev.* **1934**, *46*, 618.

(32) Frisch, M. J.; Trucks, G. W.; Schlegel, H. B.; Scuseria, G. E.; Robb, M. A.; Cheeseman, J. R.; Zakrzewski, V. G.; Montgomery, J. A., Jr.; Stratmann, R. E.; Burant, J. C.; Dapprich, S.; Millam, J. M.; Daniels, A. D.; Kudin, K. N.; Strain, M. C.; Farkas, O.; Tomasi, J.; Barone, V.; Cossi, M.; Cammi, R.; Mennucci, B.; Pomelli, C.; Adamo, C.; Clifford, S.; Ochterski, J.; Petersson, G. A.; Ayala, P. Y.; Cui, Q.; Morokuma, K.; Rabuck, A. D.; Raghavachari, K.; Foresman, J. B.; Cioslowski, J.; Ortiz, J. V.; Stefanov, B. B.; Liu, G.; Liashenko, A.; Piskorz, P.; Komaromi, I.; Gomperts, R.; Martin, R. L.; Fox, D. J.; Keith, T.; Al-Laham, M. A.; Peng, C. Y.; Nanayakkara, A.; Gonzalez, C.; Challacombe, M.; Gill, P. M. W.; Johnson, B.; Chen, W.; Wong, M. W.; Andres, J. L.; Gonzalez, C.; Head-Gordon, M.; Replogle, E. S.; Pople, J. A. *Gaussian 98*, Revision A.5; Gaussian Inc.: Pittsburgh, PA, 1998.

(33) Bergner, A.; Dolg, M.; Küchle, W.; Stoll, H.; Preuss, H. *Mol. Phys.* **1993**, *80*, 1431.

(34) Andzelm, J.; Huzinaga, S.; Klobukowski, M.; Radzio, E.; Sakai, Y.; Tatekawi, H. *Gaussian Basis Sets for Molecular Calculations*; Elsevier: Amsterdam, 1984.

(35) Boys, S. F.; Bernardi, F. *Mol. Phys.* **1970**, *19*, 553.
(36) Glendening, E. D.; Badenhoop, J. K.; Reed, A. E.; Carpenter, J. E.; Bohmann, J. A.; Morales, C. M.; Weinhold, F. *NBO 5.0*; Theoretical Chemistry Institute, University of Wisconsin: Madison, 2001.
(37) Takagi, K.; Oka, T. *J. Phys. Soc. Jpn.* **1963**, *18*, 1174.
(38) Harmony, M. D.; Laurie, V. W.; Kuczkowski, R. L.; Schwendeman, R. H.; Ramsay, D. A.; Lovas, F. J.; Lafferty, W. J.; Maki, A. G. *J. Phys. Chem. Ref. Data* **1979**, *8*, 619.
(39) Miller, R. F.; Curl, R. F. *J. Chem. Phys.* **1961**, *34*, 1847.
(40) Davis, R. W.; Gerry, M. C. L. *J. Mol. Spectrosc.* **1983**, *97*, 117.
(41) Hargittai, M.; Hargittai, I. *Int. J. Quantum Chem.* **1992**, *44*, 1057−1067.
(42) All our calculations searching for the missing structures of the other formaldehyde derivatives converged to one of dimers **III**−**VI**.
(43) 12 kJ/mol, from MP2/6-31+G* calculations.
(44) Turi, L. *Chem. Phys. Lett.* **1997**, *275*, 35−39.
(45) Rappé, A. K.; Bernstein, E. R. *J. Phys. Chem. A* **2000**, *104*, 6117−6128.
(46) Schwenke, D. W.; Truhlar, D. G. *J. Chem. Phys.* **1985**, *82*, 2418.
(47) Frisch, M. J.; Bene, J. E. D.; Binkley, J. S.; Schaefer, H. F., III *J. Chem. Phys.* **1986**, *84*, 2279.
(48) Johnson, A.; Kollman, P.; Rothenberg, S. *Theor. Chim. Acta* **1973**, *29*, 49.
(49) Müller-Dethlefs, K.; Hobza, P. *Chem. Rev.* **2000**, *100*, 143−167.
(50) Simon, S.; Bertran, J.; Sodupe, M. *J. Phys. Chem. A* **2001**, *105*, 4359−4364.
(51) Novoa, J. J.; Planas, M.; Rovira, M. C. *Chem. Phys. Lett.* **1996**, *251*, 33.
(52) Chalasiñski, G.; Szczesniak, M. M. *Chem. Rev.* **1994**, *94*, 1723−1765.
(53) Newton, J. H.; Person, W. B. *J. Chem. Phys.* **1976**, *64*, 3036.
(54) Scott, A. P.; Radom, L. *J. Phys. Chem.* **1996**, *100*, 16502−16513.